JOURNAL OF MATERIALS SCIENCE 23 (1988) 1655–1659

Microhardness and polarity in $Cd_xHg_{1-x}Te$

J. F. BARBOT, G. RIVAUD, J. C. DESOYER
Laboratoire de Metallurgie Physique, U.A. 131 CNRS, Faculté des sciences, 86022 Poitiers Cedex, France

The Vickers microhardness of $Cd_xHg_{1-x}Te$ alloys has been measured at room temperature as a function of composition and of the nature of the {1 1 1} faces for different conduction types. The hardness–composition curve shows a maximum at about $x = 0.75$. On the {1 1 1} faces, it has been found that the metal face (A face) is harder than the metalloid face for all studied doping types and is related to the different mobilities of the A(g) and B(g) dislocations. This behaviour is compared with a model previously developed for hardness polarity in GaAs.

1. Introduction

Interest in the $Cd_xHg_{1-x}Te$ (CMT) ternary alloy system results from the fact that its bandgap depends on the molar fraction of CdTe and so can be adjusted from about 1.6 eV ($x = 1$) down to -0.3 eV ($x = 0$). This II–VI semiconductor compound is the most important material for infrared detection ($x = 0.2$) and for optical applications ($x = 0.7$).

The CMT compound crystallizes in the sphalerite structure and therefore does not have a centre of symmetry. The (1 1 1) faces will terminate either with Group II atoms (A face) or with Group VI atoms (B face) and generally exhibit a different chemical reactivity and other properties.

Dislocations in II–VI semiconductors can be classified into two types depending on whether the atoms of the dislocation core are of Type II or Type VI (of the glide set). A dislocation with Type II atoms in the core is designed A(g) and similarly, a dislocation may be B(g) if the dislocation core is of Type VI.

Microindentation is the most commonly used technique for studying the low-temperature deformation characteristics of brittle materials. Previously hardness curves have been carried out against composition, but are generally incomplete or inaccurate [1–4]. For some compositions, the hardness has also been measured as a function of temperature [5, 6]. These results can be varied according to the crystal growth process.

The present work is a study of microhardness on CMT, grown by the travelling heater method (THM), as a function of composition, of face polarity (A or B) and conduction type, at room temperature. In addition, dislocation rosettes introduced by Vickers microhardness indentation have been revealed on {1 1 1}-oriented faces.

2. Experimental procedure

Two series of experiments were performed on single CMT crystals: the first one on specimens without specified orientation and the second one on {1 1 1} oriented specimens. On {1 1 1}-oriented samples, the A and B faces were determined from their etching behaviour. The etch reveals pits on the A face and not on the B face, which remains featureless or oxidized [7, 8]. So, the surfaces were mechanically and chemically polished to remove surface work damage. Microhardness tests were performed using a Vickers indenter system with a diamond pyramid. In order to observe dislocation etch-pit patterns under the indenter successive surface layers were chemically removed.

The composition was controlled by infrared (IR) optical transmission and the homogeneity obtained by IR optical cartography. Electrical characterization was made by Hall measurements at 77 and 300 K.

3. Hardness results

3.1. Variation with composition

The hardness curve obtained for 50 g indentation is shown as function of the CdTe fraction in Fig. 1, as well as various data taken from the literature (results for 80 g followed the same pattern). The samples were prepared without paying any attention to their orientation and conduction type.

The general shape of the CMT curve is in agreement with most of the previous results. The curve shows a maximum for $x = 0.75$ (1 atom of mercury for 3 atoms of cadmium) as commonly observed (or predicted) in many pseudo-binary solid solutions. In the composition range $x = 0.6$ to 0.9, the great number of specimens studied, in contrast to previous work, permit us to define exactly the peak position as well as its width.

An ordered structure in the metallic sublattice has been suggested by Balagurova and Khabaro [3] for CMT solid solutions at a composition ratio 3 : 1 or 1 : 3. In HgZnTe (MZT) solid solutions, this ordering seems to have been seen [4, 9], but there is no documented evidence for ordering in the CMT system. X-ray measurements have been carried out on CMT ($x = 0.7$); the reflections which are forbidden by the extinction law for lattices of the sphalerite structure do not appear. Therefore we can conclude that no long-range order has been observed in our solid solution.

3.2. Hardness on {1 1 1} faces

Microhardness measurements for 50 g indentation have been carried out for some compositions and

0022–2461/88 $03.00 + .12

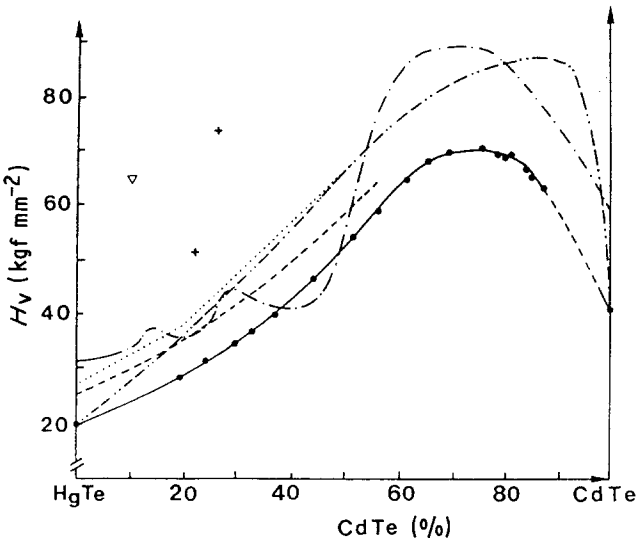

Figure 1 Microhardness curves of $Cd_xHg_{1-x}Te$ as function of composition x. (···) Cole *et al.* [1], (– – –) Sharma *et al.* [2], (– – –) Balagurova and Khabaro [3], (– – – –) Triboulet [4], (▽) Kurilo *et al.* [5], (+) Koman and Pashovskii [6], (——) Present work.

doping types on the A and B faces of {1 1 1} CMT oriented specimens at room temperature. These results are shown in Table I.

In all the cases studied, the A face is harder than the B face. This hardness difference, small for $x = 0.2$ and $x = 1$ (CdTe), becomes more important for $x = 0.7$. At $x = 0.23$ we have shown a doping-type influence; the p-type specimen seems to be a little harder than the others. The growth technique used (THM) does not permit the obtention of n-type CMT with a high concentration of CdTe; thus for $x = 0.7$ only the p-type has been studied.

4. Dislocation etching

Four samples have been studied: the A faces of n- and p-type for $x = 0.23$ and the p-type for $x = 0.7$ and $x = 1$ (CdTe). As mentioned in Section 2, it was not possible to study the B faces. Under the same experimental conditions (equal indentation load 30 g and time 15 sec) the samples were etched to reveal rosettes around the indentation.

4.1. Results for $x = 0.23$

Etch-pit rosettes in n-type (Fig. 2) are the same as in p-type CMT (Fig. 3), therefore they are not doping-type dependent. The weak hardness difference noticed in Table I between both samples is not obvious. The dislocation density is very high, thus only general data on the dislocation configuration can be obtained. The etch-pit rosettes consist of six arms and exhibit approximate threefold symmetry along ⟨1 1 0⟩ directions, i.e. the traces of {1 1 1} slip planes. Two equilateral triangles rotated against each other through an angle of 180° are also formed by the etch pits and are independent of the Vickers indenter orientation. With an indentation load of 60 g, cracks are visible along ⟨1 1 2⟩ directions, implying that they are parallel to the {1 1 0} cleavage plane.

On both specimens, dislocation etch-pit patterns have been revealed at different depths from the indentation surface. Fig. 4 shows the etched A face (n-type) at depths of 15, 20, 60 and 70 μm, to be compared with the pattern on the indentation surface (Fig. 2). No difference could be noticed between both conduction types.

At a depth of 15 μm (Fig. 4a), the etch-pit rosette arms are a little shorter. After the removal of another surface layer of 15 μm, they completely vanish (Fig. 4b), only both triangles remain. They interpenetrate and approximately have the same dimensions; the initially larger one decreases in size with increasing distance from the surface, while the other one increases. At a depth of 60 μm we note that the decreasing triangle in fact consists of a series of triangles embodied in one another. At a larger depth, 70 μm (Fig. 4c), most of these embodied triangles have disappeared. After removing a layer deeper than 90 μm thick, the triangles have completely vanished and we only observe as-grown dislocations.

TABLE I Hardness values on {1 1 1} faces of investigated samples

x	Conduction type	A	B
0.23	Intrinsic	33 ± 1	32 ± 1
	p (2×10^{17} cm^{-3})	34 ± 1	32 ± 1
	n (1.5×10^{17} cm^{-3})	33 ± 1	32 ± 1
0.2	n (1.5×10^{17} cm^{-3})	31 ± 1	30 ± 1
0.7	p (1.7×10^{15} cm^{-3})	71 ± 2	67 ± 2
1	p	37.5 ± 0.5	37 ± 0.5

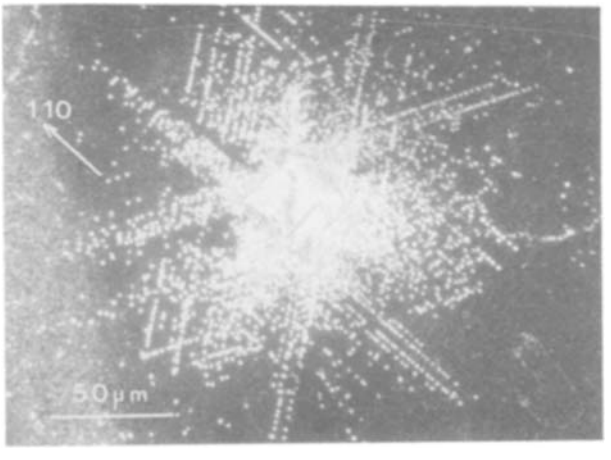

Figure 2 Etch-pit picture on n-type CMT ($x = 0.23$).

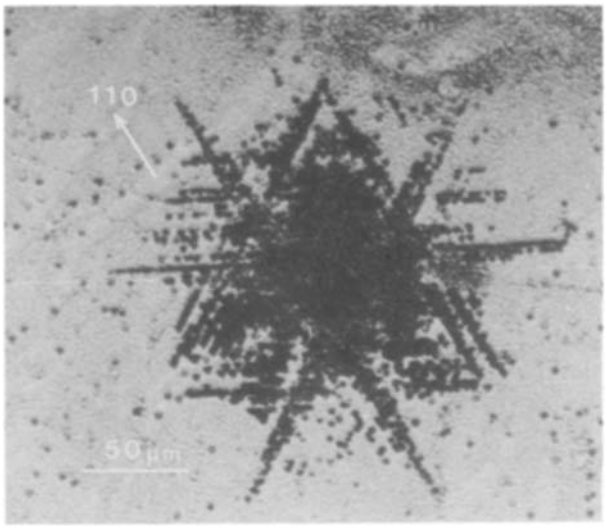

Figure 3 Etch-pit picture on p-type CMT ($x = 0.23$).

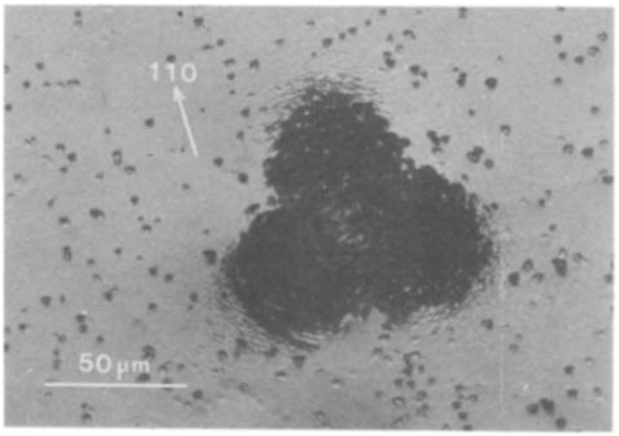

Figure 5 Etch-pit picture on p-type CMT ($x = 0.7$).

4.2. Results for $x = 0.7$

Fig. 5 shows etch pits revealed on p-type CMT ($x = 0.7$). The dislocations are closely located to the proximity of the indentation in $\langle 1\,1\,0 \rangle$ directions, showing that dislocation motion is very difficult at room temperature ($T \sim 0.26 T_m$). This result agrees with the one found in a previous study [10] suggesting that CMT ($x = 0.66$) did not exhibit any plastic flow deformation in compression tests performed at room temperature. The extension of dislocation loops should be possible by indentation at higher temperatures in order to relieve the stress field induced by compression of the material.

4.3. Results for CdTe ($x = 1$)

We only notice the two equilateral triangles formed by the etch pits in $\langle 1\,1\,0 \rangle$ directions. No long etch-pit arms as those observed by Braun *et al.* [11] are revealed for p-type CdTe. This discrepancy should be provided by the material used and there may also be some differences in the experimental conditions.

5. Discussion

It will be interesting to compare our results for the CMT alloys with the model developed by Hirsch *et al.* [12] for the $\{1\,1\,1\}$ GaAs faces at 350° C. In general the model predicts that if a compound AB has faster A(g) dislocations than B(g) dislocations, the $\{1\,1\,1\}$ surface terminating in B atoms will be harder.

By etching deformed CdTe samples, Petrenko and

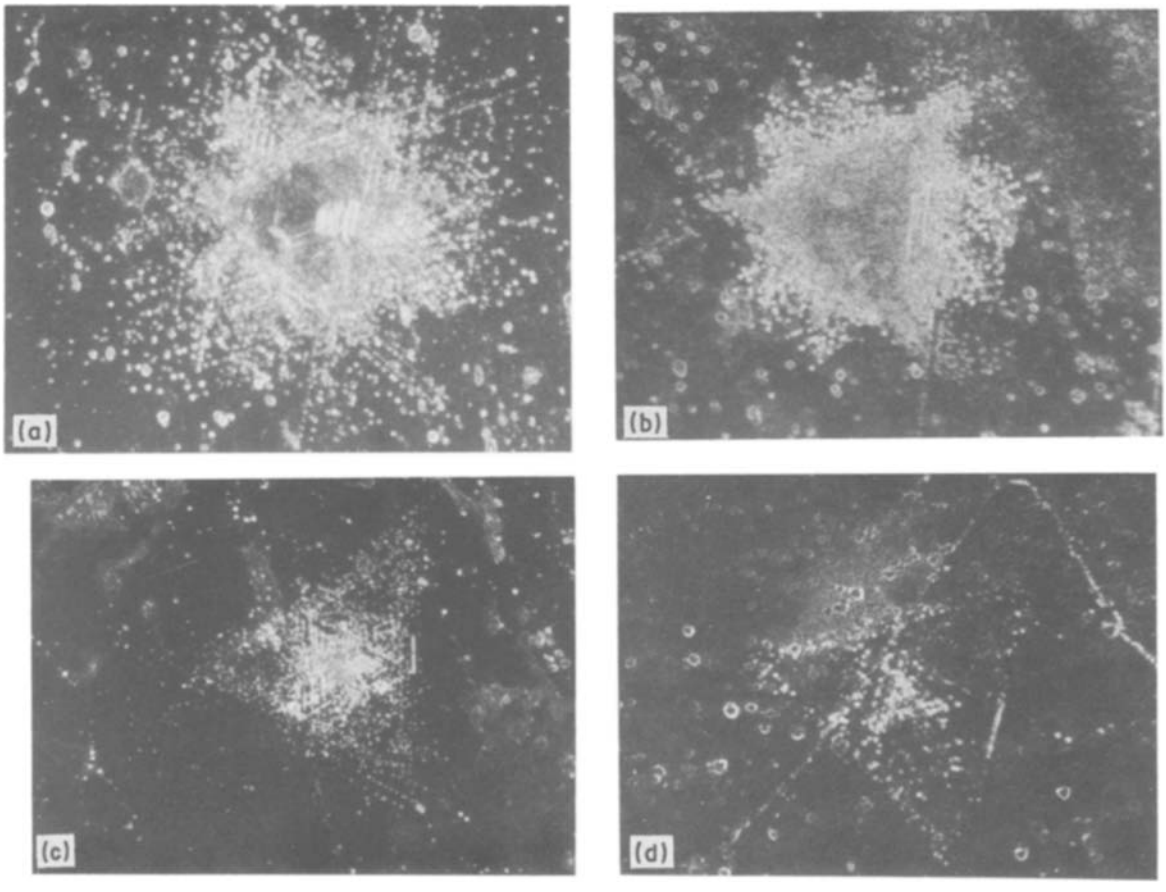

Figure 4 Etch-pit patterns at depth of (a) 15, (b) 20, (c) 60 and (d) 70 μm from the surface (for scale, see Fig. 2).

co-workers [13, 14] have observed that the Te(g) dislocations were more mobile. So, according to the Hirsch model, the A face should be harder, as we observe experimentally (Table I). The polarity of hardness of the {1 1 1} CMT faces can be explained by the same argument. The A face is harder than the B face because the B(g) dislocations are faster.

In the range of $x = 0.23$, we find that the rosette sizes are the same for n- and p-doped CMT, suggesting that the dislocation velocities are independent of the doping-type, in contrast to the situation observed in silicon by Roberts *et al.* [15]. The microhardness seems also to be doping-type independent.

Moreover, we note that this hardness difference, small for $x \sim 0.2$ and CdTe (within the limit of experimental errors), becomes more important for $x = 0.7$. These results agree with previous work on II–VI semiconductors [14]. Indeed, as a general rule, the B(g) dislocations have the higher mobility in the sphalerite structures, and the degree of asymmetry increases with higher flow stress.

However, the etch-pit picture obtained on the A faces of CMT ($x = 0.23$) does not agree with the correlation established by Hirsch *et al.* [12] on GaAs. They have observed two etch-pit picture types (see Table II), Type I corresponding to the hardest faces and Type II to the softest faces, while we observe on the harder faces (i.e. the A faces) the Type II only. The asymmetry of the dislocation mobilities is less than for GaAs because a smaller polarity in hardness is observed, and it does not influence the recovery slip, i.e. the etch-pit picture type. So, we find ourselves in a situation near to the one observed in silicon at 400° C by Eremenko and Nikitenko [16], i.e. an etch-pit picture of Type II.

Moreover, assuming that the crystallographic polarity of Fewster and Whiffen [8] is correct, Braun *et al.* [11] have shown, in contrast to our work, that the fast dislocations in CdTe are of the Cd(g) type.

Underneath the indention mark, close observations show that the dislocations slip along {1 1 1} planes and give rise to two symmetrical tetrahedra (see Fig. 6), the apices of which are respectively inside and outside the {1 1 1} surface. The inner triangles of etch pits observed in Fig. 4c, characteristic of slip on the internal apex tetrahedron, are likely to be associated with a plastic recovery process, occuring after the indenter is removed, as suggested by Hirsch *et al.* [12]. Indeed, if these inner triangles are extrapolated to the surface, the resulting width is quite comparable to that of surface triangles. Because of the formation of Lomer–Cottrell locks, the slip on the internal apex tetrahedron is limited and the total arrangement consists of series of these tetrahedra, one sitting inside another.

TABLE II Hardness values and etch-pit picture types for GaAs at 350° C (from Hirsch *et al.* [12])

Type	H_V (MPa)		Picture type	
	A (III)	B (V)	A(III)	B(V)
n	3000	2300	I	II
p	2200	2600	II	I

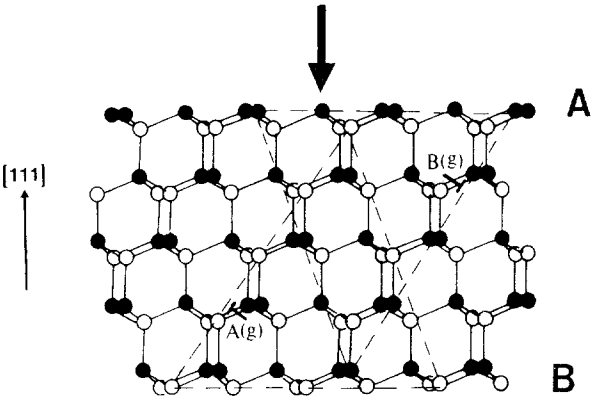

Figure 6 Slip on the two tetrahedra for an indentation on the A face.

The difference in penetration of these two tetrahedra, due to the asymmetry of the dislocation mobilities, observed on GaAs, has not been seen on CMT ($x = 0.2$), probably because of the weak difference in the dislocation mobilities.

The loops that form rosette arms are rather shallow (Figs 4a and b). Thus, the screw dislocations which control the depth of the rosette are slow.

6. Conclusion

The Vickers hardness–composition curve exhibits a peak for $x = 0.75$ at 293 K. This is typical of a binary solid solution system. We have not observed evidence of ordering at this composition.

The hardness polarity behaviour on {1 1 1} CMT faces is explained in terms of dislocation mobilities. Thus, the B(g) dislocations have been found to be faster than the A(g) dislocations. Therefore, this mobility difference should be weak.

Acknowledgements

Mm. Durand, Dessus and Lescoul (SAT, Poitiers) are acknowledged for providing CMT single crystals.

References

1. S. COLE, M. BROWN and A. F. W. WILLOUGHBY, *J. Mater. Sci.* **17** (1982) 2061.
2. B. B. SHARMA, S. K. MEHTA and W. V. AGASHE, *Phys. status solidi (a)* **60** (1980) K105.
3. E. A. BALAGUROVA and E. KHABARO, *J. Sov. Phys.* **7** (1976) 943.
4. R. TRIBOULET, private communication (1987).
5. I. V. KURILO, I. M. SPITKOVSKII and A. D. SHNEIDER, *Izv. Uvz. Fizika* **9** (1974) 130.
6. B. P. KOMAN and M. V. PASHOVSKII, *Ukr. Fizika. Zh.* **23** (1978) 58.
7. S. G. PARKER and J. E. PINNEL, *J. Electrochem. Soc.* **118** (1971) 1868.
8. P. F. FEWSTER and P. A. C. WHIFFIN, *J. Appl. Phys.* **54** (1983) 4668.
9. B. TOULOUSE, R. GRANGER, S. ROLLAND and R. TRIBOULET, *ibid.* **48** (1987) 247.
10. J. F. BARBOT, G. RIVAUD and J. C. DESOYER, in Proceedings of 14th International Conference on Defects in Semiconductors, Paris, August 1986, edited by H. J. Von Bardeleben, Vol. 10–12, Part 2, p. 809.
11. C. BRAUN, H. W. HELBERG and A. GEORGE, *Phil. Mag. A* **53** (1986) 277.
12. P. B. HIRSCH, P. PIROUZ, S. G. ROBERTS and P. D. WARREN, *Phil. Mag. B* **52** (1985) 759.
13. V. F. PETRENKO and R. W. WHITWORTH, *Phil.*

Mag. A **41** (1980) 681.
14. Y. A. OSIP'YAN, V. F. PETRENKO, A. V. ZARETSKII and R. W. WHITWORTH, *Adv. Phys.* **35** (1986) 115.
15. S. G. ROBERTS, P. PIROUZ and P. B. HIRSCH, *J. Physique Coll.* **44** (1983) C4-75.
16. V. G. EREMENKO and V. I. NIKITENKO, *Phys. Status Solidi (a)* **14** (1972) 317.

Received 14 May
and accepted 22 October 1987